scientific reports

Check for updates

OPEN

Predicting creep failure life in adhesive-bonded single-lap joints using machine learning

Faizullah Jan[1], Marcin Kujawa[1]✉, Piotr Paczos[2] & Victor A. Eremeyev[3]

Accurately predicting the creep failure life of adhesive joints, particularly single-lap adhesive joints (SLAJs), remains still a significant challenge, requiring substantial time and resources and the ability to predict the duration of creep failure in SLAJs is critical to ensuring structural integrity and reducing the failure of creep-prone adhesive joints. In this study, machine learning (ML) was used to identify the critical features that ultimately influence the durability of SLAJs due to creep. These key features were determined through correlation analysis and sequential feature selection. Multiple ML algorithms were employed to analyze complex relationships among key features and predict creep failure life. Finally, the results of the analysis highlight the importance of features such as SLAJ creep strain, adhesive tensile strength (UTS), SLAJ creep stress, adhesive surface area (*A*), and Young's modulus (*E*). Of the ML models tested, the random forest (RF) model was the most effective in predicting creep failure life. Moreover, the accuracy of the predictions made by the proposed ML model, using original code written in Python, has been verified in experimental tests. All datasets generated and analyzed during the current study, along with the code, are available in the repository accompanying the paper.

Keywords Single-lap adhesive joints, Creep failure life, Machine learning, Random forest model, Experimental studies

In recent decades, structural adhesives have gained prominence in the aerospace, automotive, marine, and civil engineering industries due to their numerous advantages. For instance, in metal structures, adhesives can replace conventional mechanical fasteners such as bolts and welds. This substitution reduces stress concentrations, ensures a uniform distribution of stress across the joint, minimizes corrosion and vibration, and decreases the overall weight of the structure[1–3]. However, structural adhesives also have certain disadvantages. For example, due to their viscoelastic behavior, they may exhibit creep deformation when subjected to prolonged loading, even at ambient temperatures[4–6].

The phenomenon of creep must always be considered to ensure the long-term structural integrity of bonded joints, particularly in cases involving thicker adhesive layers. Creep in bonded joints is a complex process influenced by various factors, including temperature, humidity, adhesive composition, substrate properties, bonding element characteristics, and other contributing variables. Three major creep regions are observed following the instantaneous elastic strain that occurs when a load is applied to the material[7,8]. These regions are primary creep, characterized by a nonlinear and initially high rate of creep strain that decreases over time, secondary creep, during which the creep strain rate remains steady, and tertiary creep, defined by a rapid acceleration in the creep strain rate that ultimately results in material failure[9]. Creep is undoubtedly a complex, time-dependent phenomenon[10,11], which makes predicting the durability of finished products particularly challenging. Standard laboratory experiments dedicated to studying creep are both time-consuming and costly[12]. Nevertheless, evaluating durability under creep conditions remains essential for design purposes. Consequently, designers and contractors continue to seek simple methods for assessing the effects of creep on bonded joints to ensure the optimal durability of structures under prolonged loading conditions[13].

Various methods have been employed in the past to simplify the estimation of creep in bonded joints. However, these methods often fail to accurately represent the creep behavior over the long-term service life of bonded joints[11]. Early approaches included experimental testing methods, such as conducting tests at temperatures significantly higher than the operating temperature. While these methods provided useful insights, they were effective only for short time periods[14]. On the other hand, various analytical and numerical models have been employed to characterize the behavior of viscoelastic structural adhesives. For instance, power-law

[1]Gdańsk University of Technology, G. Narutowicza 11/12, 80-233 Gdańsk, Poland. [2]Poznań University of Technology, Jana Pawła II 24, 61-139 Poznań, Poland. [3]University of Cagliari, Via Marengo 2, 09123 Cagliari, Italy. ✉email: marcin.kujawa@pg.edu.pl

models initially perform well but fail to capture long-term behavior. Subsequently, models such as Maxwell, Kelvin-Voigt, and Burgers, which are based on combinations of springs and dashpots, offer greater flexibility and allow for the fitting of more complex composite creep data. The Kohlrausch-Williams-Watts (KWW) equation, which describes the viscoelasticity of polymers using a fractional exponential distribution, is also occasionally applied[15].

The time-temperature superposition (TTS) method is another widely used approach, particularly for evaluating the viscoelastic properties of epoxy adhesives. This method, first introduced by Leaderman[16], combines data obtained at different temperatures to construct a master curve representing creep behavior over time. The fundamental premise of this method is that, for many materials, the relationship between logarithmic time and creep compliance remains consistent across various temperatures[11]. Consequently, the principle of time-temperature superposition utilizes the concept of reduced time and has been employed for long-term creep predictions. For example, Feng et al.[15] applied this method by fitting creep data using a physics-based model and the TTS method to generate a master curve for determining long-term creep behavior. Similarly, Marques et al.[11] used this approach to estimate creep failure in aluminum-glass adhesive joints.

Shi et al.[17], on the other hand, utilized various models, including the previously mentioned Burgers and Kelvin-Voigt models, to predict creep coefficients in timber structures with bonded steel plate joints. Their work also aimed to anticipate joint creep slip over the service life of such systems. Over the past century, numerous models have been developed to predict the creep life of polymers and alloys. These include the time-temperature parameter method, Robinson's linear rule, the damage parameter method based on creep damage mechanics, and prediction techniques based on creep curves, such as the θ-projection and the Ω-method[18]. Unfortunately, conventional methods remain limited in practical application due to their reliance on short-term data and complex theoretical frameworks. Furthermore, creep experiments, which are crucial for designing adhesive joints, are inherently time-consuming. Additionally, factors such as temperature fluctuations, variable creep mechanisms, and material differences[11] mean that both computational and experimental methods often yield only approximate results. As a result, many researchers have shifted away from traditional creep testing methodologies, focusing instead on the statistical analysis of material data. Consequently, conventional models for predicting creep durability now have somewhat restricted practical applications.

Hence, recent ML methods based on statistical data have shown potential in predicting the service life of components[19,20], along with the development of material behavior simulation. ML captures complex nonlinear relationships between environmental and material data at a large scale, providing a viable alternative to traditional prediction methods and overcoming their limitations. Currently, various ML methods, such as Multi-Layer Perceptron (MLP)[21], linear regression[22], Random Forest (RF)[18,23], Deep Neural Networks (DNN)[24], and ensemble methods[25–27], are being used to accurately capture the complex correlations between a wide range of material characterization data, environmental factors, and stress (as inputs), and creep durability (as the output). For example, Chai et al.[19] highlight significant advances in ML for predicting alloy creep damage. Zhang et al.[24] introduced DNN to predict complex creep and fatigue damage in stainless steel. Meanwhile, Tan et al.[28] investigated ensemble ML methods, including additional trees and eXtreme Gradient Boosting (XGB), to improve the prediction of creep life in Cr martensitic steel. In contrast, Yue Liu et al.[26] proposed self-adaptive ML methods to accelerate the prediction of creep life in improved nickel-based alloys, providing valuable information for future research. Shin et al.[29] used the maximum information coefficient (MIC) and Pearson correlation coefficient (PCC) to correlate input features, generated by computational methods, with creep durability. Verma et al.[22] proposed ML methods, such as linear regression and lasso regression, as well as t-distributed stochastic neighbor embedding (t-SNE), to relate microstructure to creep properties of chromium steels. Additionally, ML has wide applications in materials science, including predicting mechanical properties[30–32], evaluating physical properties[33,34], analyzing material microstructures[35,36], and designing advanced materials[37,38].

As can be seen, ML has a wide range of applications in materials science, including the prediction of mechanical properties[30–32], the evaluation of physical properties[33,34], the analysis of material microstructures[35,36], and the design of advanced materials[37,38].

This study employs the dataset available in the literature: Queiroz et al.[39], Tan et al.[40], Zeeuw et al.[41], and Duncan et al.[42], to construct a reliable and accurate ML model that identifies key features through feature screening and predicts the creep life of adhesive-bonded single-lap joints. Multiple ML algorithms, including ridge and lasso regression, support vector regression, and Gaussian process regression, are employed in conjunction with RF and DT in the model's training to evaluate their impact on prediction accuracy. Additionally, the proposed ML model has been validated through experimental studies.

While the algorithms and datasets utilized in this study build upon previous scientific achievements, it is important to highlight the innovative approach taken in applying and validating these resources to address the specific challenge of predicting the durability of single-lap joint creep damage. Specifically, independent feature selection and correlation analyses were performed to identify the most critical predictors, a tailored ML framework is developed to enhance predictive accuracy, and the model is validated through experimental testing. These efforts successfully demonstrate the feasibility of integrating ML with an understanding of bonded joint behavior under creep conditions.

Methodology

The main objective of this study is to develop a reliable ML model for predicting the creep failure life of SLAJs by identifying key features from a diverse dataset. Figure 1 illustrates the ML framework used in this study, which includes data preprocessing, feature selection, model training, model evaluation, and, finally, prediction along with its application.

Our dataset (see Table 1) contains input features from experimental tests that are related to the output feature, which is creep durability. We preprocessed the data sequentially to improve the accuracy of the ML model. This

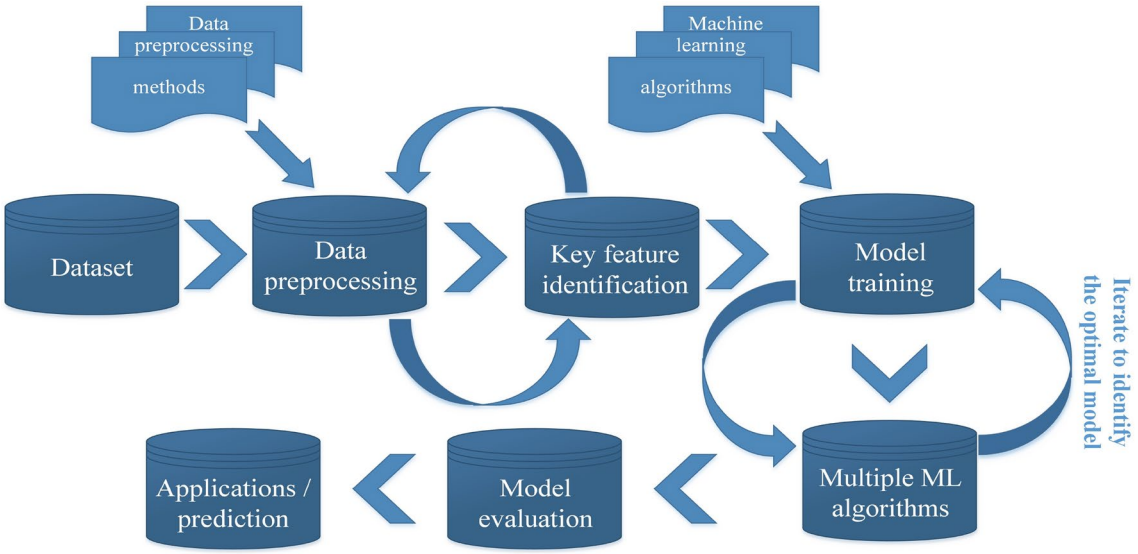

Figure 1. ML framework for predicting creep failure life.

Test	References	Types of adhesives	Datasets	Adherend
1	Queiroz et al.	Epoxy	4	Steel (ASTM A-36)
		Polyurethane	6	
2	Tan et al.	Polyurethane Sikaflex 265	62	Aluminum (6005A)
3	Zeeuw et al.	Epoxy Araldite 2015,	30	Steel (S700MC)
4	Duncan et al.	Polyurethane DP609	126	Steel
		Elastomer Evode M70	57	

Table 1. Creep life dataset obtained in single-lap joint tests.

process included normalizing the input features to a range of 0 to 1 and applying a logarithmic transformation to the output dataset. Feature pre-selection identifies key features that impact the model's predictive accuracy through correlation analysis and sequential selection. Additionally, it streamlines the model by removing "unnecessary" features[43]. After identifying the critical features, several ML models are utilized to train the model using *k*-fold cross-validation. Next, the most reliable model is selected for additional analysis, and key evaluation metrics, including the coefficient of determination (R^2) and the Root Mean Square Error (RMSE), are computed. Ultimately, this model can predict creep failure life based on future data, facilitating comparisons with real-world values. The analysis aimed at predicting the durability of creep damage in adhesive joints has focused on mechanical properties rather than on chemical composition or environmental factors.

Collection of data

This research emphasizes data related to mechanical properties, as they have a direct impact on the durability of joints. Given their critical role in evaluating creep durability, the input variables primarily focus on these properties. A total of 285 datasets were collected, comprising 34 for epoxy adhesives, 194 for polyurethane adhesives, and 57 for elastomer adhesives. Tables 1 and 2 present the distribution of the collected datasets, which include experimental results from four different studies on the creep failure life of adhesively bonded single-lap joints. At this point, it is important to emphasize that the limitations of the proposed model are primarily attributable to the size and quality of the dataset. The data presented in Table 2 were selected to represent a wide range of properties of structural adhesives used in various engineering applications. The selection was based on the criteria of availability in the scientific literature and suitability for statistical analysis and modeling. Due to the limited access to homogeneous experimental data, results from different sources were utilized, which may have introduced significant variation in the values of individual parameters. While the dataset does not encompass the full spectrum of available adhesives, it captures key mechanical and physical properties relevant to creep phenomena. The model proposed in this study, utilizing datasets covering different types of adhesives, aims to create a universal tool that is not restricted to any single adhesive type. Accordingly, the model was designed to account for variations in creep durability across different adhesives. Figure 2 illustrates example data showing the variation in creep life for different adhesives as influenced by the ultimate shear strength of SLAJs.

Obviously, a larger dataset would increase the accuracy of the model. However, gathering such an extensive database is not an easy task and requires time. Nevertheless, the datasets used in this study are sufficiently adequate for predicting durability in creep failures. In this study, the dataset collected includes eleven input

Data	Abbreviation	Description	Min.	Max.	Mean	SD
Inputs	USS [MPa]	Ultimate shear strength of SLAJ	4.5	20	10.86	5.72
	UTS [MPa]	Ultimate tensile strength of adhesive	1.61	40	14.79	10.21
	E [MPa]	Young's modulus of adhesive	2.7	1600	308.60	488.66
	G [MPa]	Shear modulus of adhesive	0.7	1960	231.87	314.01
	ν [-]	Poisson's ratio of adhesive	0.32	0.39	0.35	0.01
	Creep strain [-]	Creep strain of SLAJ	0.0028	1.54	0.19	0.28
	Creep stress [MPa]	Creep stress of SLAJ	0.24	14.1	1.53	2.20
	Temperature [°C]	Testing temperature	20	80	35.15	24.40
	RH [%]	Relative humidity	50	95	62.56	11.55
	t [mm]	Thickness of adhesive	0.5	1	0.66	0.23
	A [mm^2]	Area of adhesive	312.5	625	414.00	145.72
Outputs	Creep failure life [hr]	Time from creep to failure	0.0025	2334	57.59	188.35
	Log[CreepLife]	Creep life in logarithmic form	-2.58	3.36	0.69	1.10

Table 2. Summary of statistical analysis of collected input and output features.

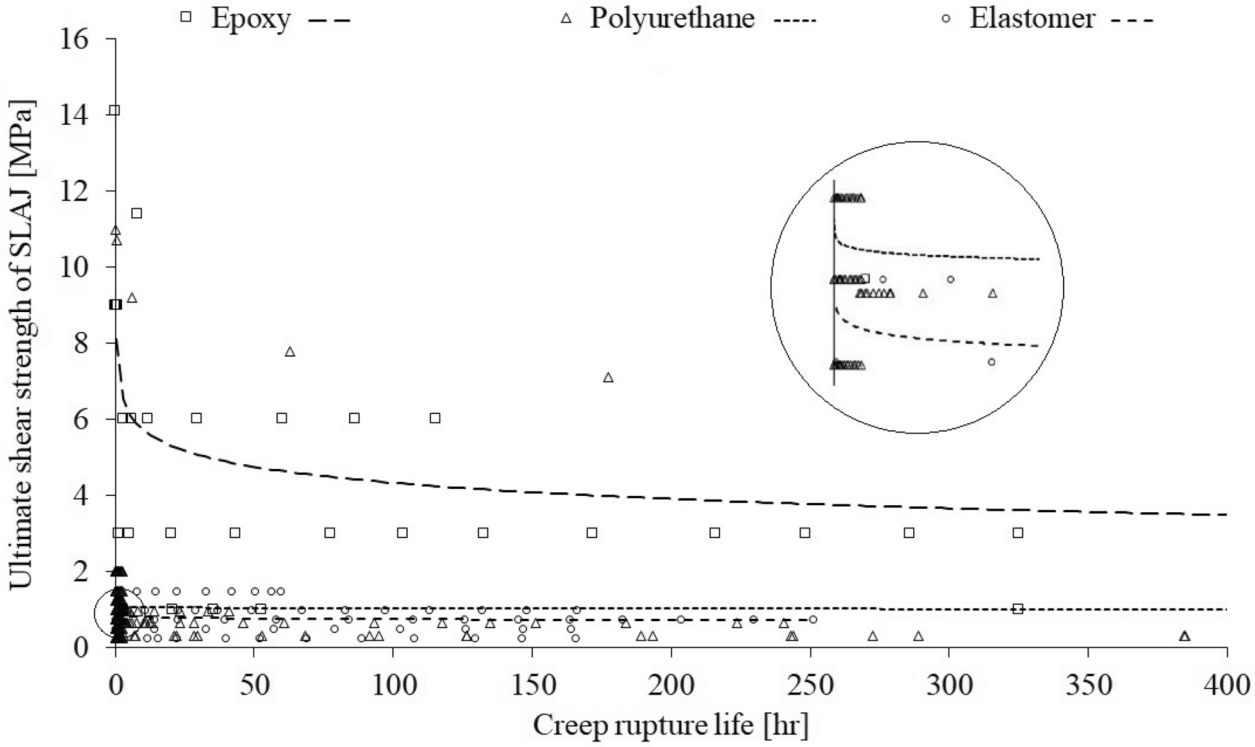

Figure 2. Logarithmic trend lines based on ultimate shear strength of SLAJs for variation in creep failure life for different adhesives[39–42].

features and a single output feature, which is the average creep time in hours [hr]. The input features include the following elements: 1) ultimate shear strength of SLAJ (USS), 2) ultimate tensile strength of the adhesive (UTS), 3) Young's modulus of the adhesive (E), 4) shear modulus of the adhesive (G), 5) Poisson's ratio of the adhesive (ν), 6) creep stress in the longitudinal direction, 7) creep strain in the longitudinal direction, 8) testing temperature (T), 9) relative humidity (RH), as well as geometrical factors such as 10) adhesive thickness (t) and 11) adhesive area (A), all of which influence the creep failure life of adhesive-bonded joints. Table 2 provides a summary of the statistical analysis performed on the collected input and output features. The target feature of this study is the creep failure life, as shown in Table 2 in terms of the output data. In this study, creep life is additionally transformed into a logarithmic form, referred to as Log[CreepLife], which is a commonly used method for predicting creep properties.

Here, we would like to draw the reader's attention to two facts. First, the minimum value of the time description on the logarithmic scale, which is negative, is not incorrect. This is because this value does not directly represent

time itself, but the logarithm of the time value. The logarithm of a number can be negative when the number is less than 1 but greater than 0. In the context of time, if time is expressed in hours [hr], as in our case, and is less than 1 hour (for example, 100 seconds), then the logarithm of this value will be negative. Second, it is important to distinguish between the concept of creep damage life, as shown in Table 2, and the minimum life of adhesive joints. As noted by Marques et al.[11], the minimum life of adhesive joints is approximately 20 years, while creep life refers to the period of time a material can withstand a given load before being damaged by creep.

Data preprocessing

The input and output features exhibit varying degrees of deviation, as illustrated in Table 2, with the creep failure life being broadly distributed and having a very high standard deviation. To mitigate the issues caused by the notable variation in feature ranges, input variables were standardized to fall between 0 and 1. Data standardization, normalization, is a technique used to scale input data values to a common range, typically between 0 and 1. The process involves subtracting the minimum value of the variable from each observation and then dividing the result by the range of the variable. Mathematically, it can be expressed as:

$$x_n = \frac{x - min(x)}{max(x) - min(x)}, \tag{1}$$

where x represents the original value, x_n is the normalized value, and $min(x)$ and $max(x)$ are the minimum and maximum values of the variable in the dataset. Normalization is particularly useful for algorithms sensitive to differences in scale or models that require faster convergence during training. By rescaling the data, all features are adjusted to the same scale, ensuring that no single variable disproportionately influences the learning process. Nevertheless, this method should be applied with caution in the presence of outliers, as extreme values can significantly affect the range and, consequently, the results of the normalization process. Furthermore, the output feature underwent a logarithmic transformation. This preprocessing streamlines the data distribution analysis and improves modeling accuracy.

Instead of using a single split to evaluate the generalization capacity of various ML models, this study employs 5-fold cross-validation. K-fold cross-validation splits the data into multiple groups for ML techniques[44], where k represents the number of data groups. In this study, $k = 5$ distinct training and testing data groups are created from a randomly shuffled dataset to ensure diversity. K-fold cross-validation is an essential method in ML that allows for better model assessment, reduces the likelihood of overfitting[21,28], and maximizes the use of the available data[45,46]. All ML models in this paper are programmed using scikit-learn in Python with the IPython kernel.

Key features identification

The primary objectives of the feature selection process are to reduce the dimensionality of input features, thereby accelerating the training process and enabling the development of a more flexible and user-friendly model. Additionally, the process aims to identify and analyze the key features that significantly influence the target variable[47,48]. In this study, sequential selection techniques and Pearson correlation analysis are employed for feature identification. The Pearson correlation analysis evaluates the strength of linear relationships between variables and serves as a primary filter during feature screening. The Pearson correlation coefficient is calculated using the following formula (2):

$$r = \frac{\sum_{j=1}^{s}(X_j - \bar{X})(Y_j - \bar{Y})}{\sqrt{\sum_{j=1}^{s}(X_j - \bar{X})^2}\sqrt{\sum_{j=1}^{s}(Y_j - \bar{Y})^2}}, \tag{2}$$

where s denotes the total number of samples in the dataset, X_j and Y_j represent the values of the features X and Y for the j-th sample, and $\bar{X}$ and $\bar{Y}$ denote the mean values of features X and Y, respectively.

Features with an absolute Pearson correlation value $|r|$ less than 0.95 are considered less influential. Conversely, features with $|r|$ greater than 0.95 are deemed linearly proportional, indicating similar effects on the output. These selected features are subsequently analyzed using the SHapley Additive ExPlanation (SHAP) method[49] to quantify their contributions to the model's predictions. The study ranks the significance of each feature for prediction and evaluates their overall impact.

The SHAP technique assesses the importance of each input feature, which is then incrementally incorporated into the regression model. Critical features are identified based on the smallest increase in the coefficient of determination (R^2) or the greatest reduction in root mean square error RMSE. These essential features are subsequently utilized to construct ML models for predicting creep failure life.

Training and evaluation of the model

A variety of ML algorithms have been tested in this study, including ridge and lasso regression, GPR, and SVR, in conjunction with RF and DT, for model training. As previously mentioned, the parameters of the regression model are optimized to maximize R^2 and minimize RMSE. The error metrics are calculated using the following formulas (3) and (4):

$$R^2 = 1 - \frac{\sum_{j=1}^{s}(y_j - \hat{y}_j)^2}{\sum_{j=1}^{s}(y_j - \bar{y})^2}, \tag{3}$$

$$\mathrm{RMSE} = \sqrt{\frac{\sum_{j=1}^{s}(y_j - \hat{y}_j)^2}{s}}, \tag{4}$$

where s denotes the overall number of data sets, $\hat{y}_j$ denotes the predicted value, y_j denotes the actual value, and $\bar{y}_j$ denotes the average of the observed data y.

The most reliable ML method for predicting creep failure life is selected based on error comparison, while the reliability of the life prediction outcomes is evaluated using the standard deviation ($\pm 2\sigma$).

Results interpretation

Analysis of results in the identification of key features

The results of the key feature identification process are presented in Fig. 3, which displays the Pearson correlation coefficients as a grayscale map: positive correlations are shown in black, and negative correlations in white. As observed in Fig. 3, most of the computed Pearson coefficients are below 0.95, indicating nonlinear dependencies and the independence of the dataset's features. This emphasizes the importance of accurate durability predictions in cases of creep.

Figure 4 presents SHAP values derived using the game theory approach, demonstrating the contributions of individual features to the model's predictions. Specifically, Fig. 4a ranks the features by their absolute mean SHAP values, while Fig. 4b illustrates local feature contributions on a logarithmic scale. In Fig. 4b, positive

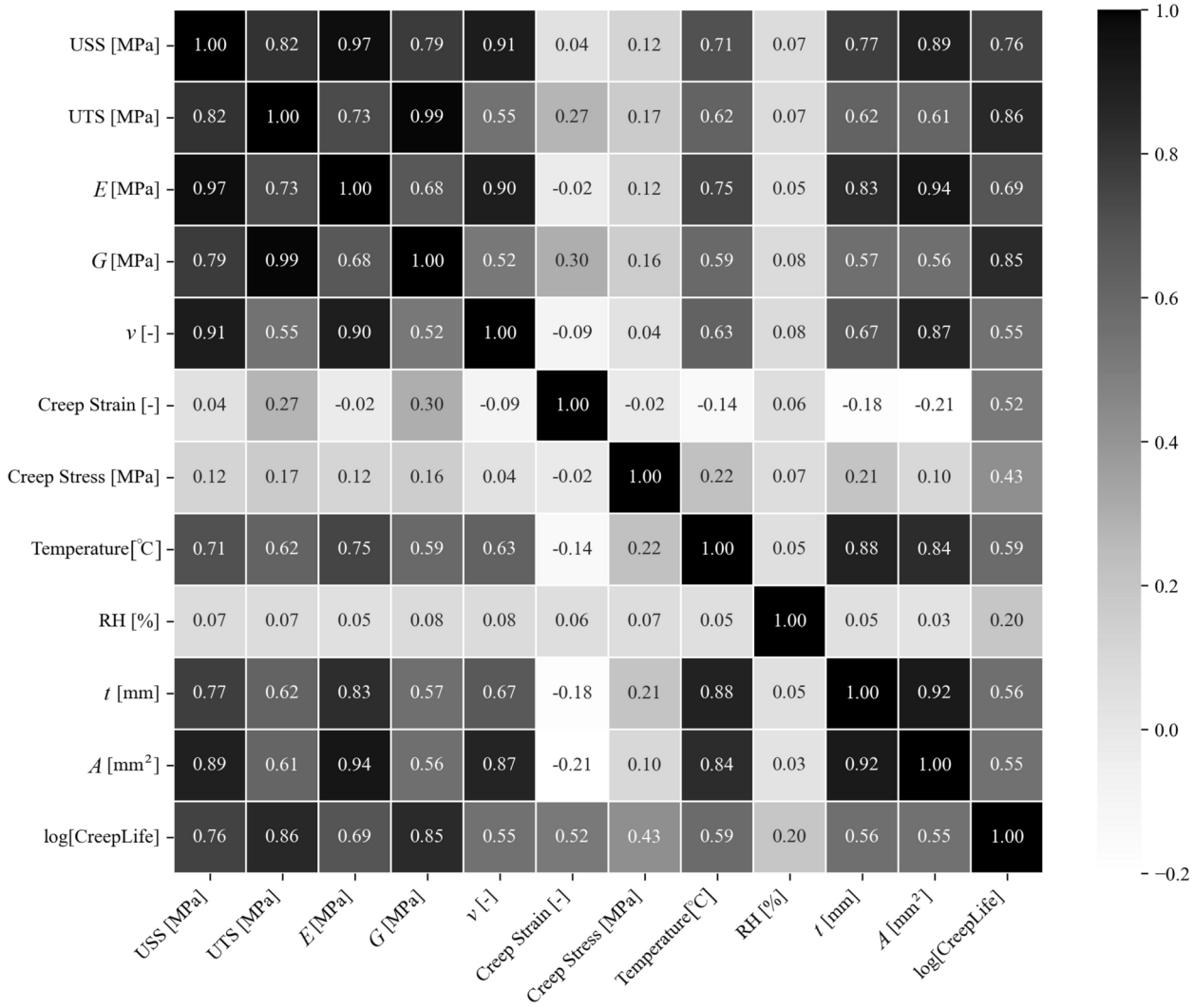

Figure 3. Map of Pearson correlation coefficients.

SHAP values indicate an increase in predicted creep failure life, whereas negative SHAP values correspond to a decrease.

As observed, the creep strain of SLAJ has the most significant positive impact on creep failure life, whereas creep stress demonstrates a substantial negative effect. While this finding is somewhat obvious and intuitive, it is important as it validates the reliability of the analyses performed. As shown in Fig. 4b, a positive SHAP value for the creep strain of SLAJ indicates that an increase in strain may lead to a longer predicted creep life. Although this outcome is not always intuitive or universally applicable, it can occur under certain conditions. Such behavior may result from material properties, such as strain hardening, or specific stress redistribution

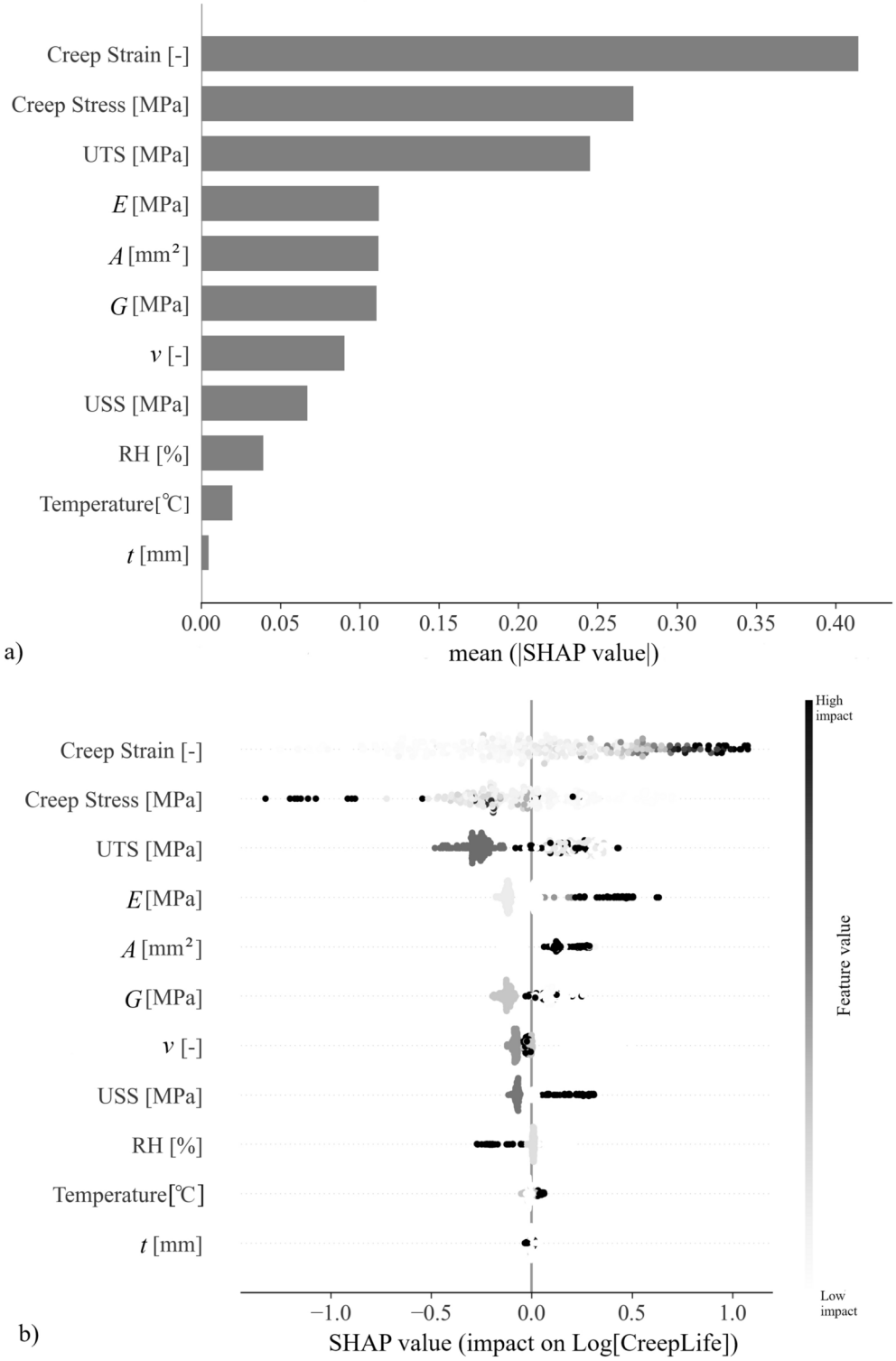

Figure 4. SHAP values: (**a**) significance of input variables, and (**b**) summary plot of SHAP values.

mechanisms that enhance creep failure life. UTS was also identified as a key feature. For this parameter, when the SHAP value is greater than 0, the UTS values are relatively high, suggesting a longer predicted creep failure life. This is because materials and structures with higher tensile and shear strengths can withstand greater stress levels before failure, thereby prolonging the period of creep deformation before failure. Similarly, the elastic modulus E of the adhesive exhibits a positive trend, akin to UTS, USS, and adhesive area A, in influencing the creep failure life of the joint. SHAP values greater than 0 for these features indicate that an increase in E, USS, or A contributes to extending creep failure life.

Other features, such as ν and G, along with testing temperature, have a lower impact on creep life, as their SHAP values are close to zero. Notably, RH is the only feature that consistently exhibits a negative effect on the behavior of the connector, which is expected. Additionally, a slight increase in testing temperature shows a minor but positive effect on the creep failure life of SLAJ.

The next Fig. 5 illustrates sequential forward selection using the GPR (Fig. 5a), SVR (Fig. 5b) and RF (Fig. 5c) models. Of these three ML models, RF achieves the highest R^2 and lowest RMSE with the fewest key features (only 4 to 5 features), after which both values plateau, indicating minimal impact on the prediction of durability in the event of creep failure life. The summary of results shown in Fig. 5 also demonstrates how the significant impact and critical importance of feature selection on performance before training and testing the ML model.

SLAJ creep strain, SLAJ creep stress, UTS, E, A followed by G, ν, and USS, are identified as the most important features, highlighting the dominance of mechanical and geometrical properties over other factors, such as environmental influences (RH, testing temperature), in determining the load-carrying capacity of SLAJs. According to the analysis, the influence of the adhesive layer thickness t is relatively insignificant, which may seem counterintuitive. However, it should be noted that the thickness ranges of adhesives (see Table 2) used in the model construction are relatively small.

In summary, the five most important input features used in the analysis to train ML models are creep strain of SLAJ, creep stress of SLAJ, ultimate tensile strength of adhesive (UTS), Young's modulus (E) and adhesive area (A). The other six features - shear modulus of the adhesive (G), Poisson's ratio (ν,) ultimate shear strength of SLAJ (USS), relative humidity (RH), testing temperature (T), and adhesive thickness (t) - are considered less important for model prediction.

Furthermore, it should be noted that our intention is not to diminish the importance of features beyond these five key ones but rather to identify trends within the specific scope of our study while considering the correlations among all features. Additionally, it is important to emphasize the interdependence of all traits and acknowledge that the process under study cannot be simplified into straightforward cause and effect relationships. Instead, it is essential to determine which factors have the most significant impact within our experimental framework, while recognizing that these findings may not fully capture the broader complexity of the underlying relationships.

Analysis of model prediction results

For the ML algorithms analyzed (lasso and ridge regression, GPR, SVR, DT, and RF), their performance in capturing complex nonlinear relationships between multiple variables and SLAJ durability under creep conditions was evaluated.

Figure 6 presents performance metrics, including R^2 and RMSE, for all these ML techniques. As previously mentioned, generalizability, which is critical in ML, is assessed using 5-fold cross-validation metrics for the analyses performed.

According to the study, the RF model outperforms other algorithms by achieving the lowest RMSE and the highest R^2 values (see Fig. 6f). This demonstrates its enhanced ability to capture complex nonlinear relationships with creep failure life. As conjectured, the performance of ridge and lasso models is inferior to other ML models because they are linear and do not account for nonlinear relationships in creep failure life (see Fig. 6a, b). As you can see in Fig. 6c, d, GPR with a Radial Basis Function kernel achieves higher accuracy than SVR with a polynomial kernel. Additionally, the DT model tends to overfit resulting in decreased accuracy. In summary, RF, as an ensemble technique, outperforms models such as DT, SVR, and GPR, as demonstrated in Fig. 6. Therefore, RF appears to be the most effective method for predicting the durability of creep failure life in single-lap adhesive joints.

Figures 7 and 8 present parity plots comparing the predicted and actual creep failure life of adhesive-bonded SLJs on a logarithmic [Log] scale and an actual time scale [hr]. The RF model, utilizing five significant input features, is employed for this comparison. Data points aligning with the 45° line, as shown in Figs. 7 and 8, indicate accuracy and are further supported by the low RMSE values observed in both the training and testing datasets. The data points, categorized by the ultimate strength of SLAJ, exhibit remarkable consistency across different ultimate strength levels. Most of the predicted data falls within the 2-factor standard deviation, confirming the accuracy and stability of the RF model, even for long-term creep data exceeding 100 h. These findings validate the RF model's satisfactory predictive accuracy and adaptability for estimating creep failure life.

Validation of ML model using experimental studies

To confirm the validity of the analyses conducted using ML, an experimental study was carried out. The six creep tests were conducted using a proprietary creep machine in the laboratory of the Gdańsk University of Technology (Figs. 9, 10). Prior to the creep tests, the average ultimate strength of the bonded joints (three samples) was examined for the tested adhesive (Zwick Z400). The obtained value of ultimate strength of SLAJ served as a reference and was regarded as the maximum load that each joint could withstand. The selected load levels for creep tests where of about 80% of ultimate strength of SLAJ. The specimens were constructed from aluminum alloy (6060 T6) and adhesively bonded using 3M Scotch-Weld DP490 adhesive. The important features like ultimate strength of SLAJ (USS), ultimate tensile strength of adhesive (UTS), E, G (value was determined from

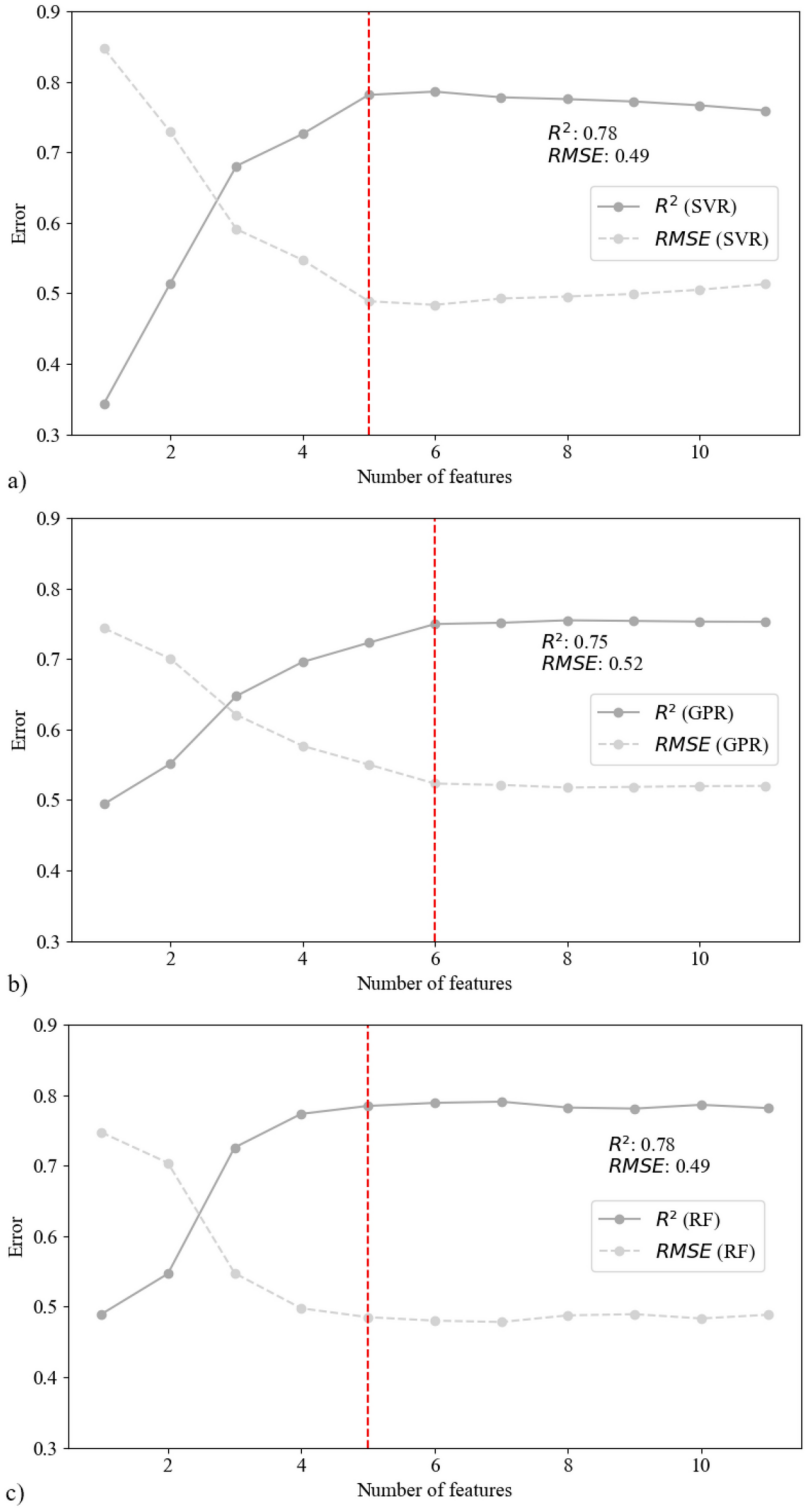

Figure 5. R^2 and RMSE variations in proportion to the quantity of input features: (**a**) Gaussian process regression model, (**b**) support vector regression model, and (**c**) random forest model.

the relationship $G = E/[2(1+\nu)]$), ν, creep strain of SLAJ, creep stress of SLAJ, testing temperature, relative humidity, and geometrical parameters were determined experimentally. These values are shown in Table 3.

The experiments conducted enabled the validation of the proposed method for predicting the creep life of the tested bonded joint. The results of this comparison are shown in Table 3. As observed for the tested samples, the results obtained from the computer program show an excellent agreement of 3.2%, with an absolute error of only 0.07 h, which corresponds to a difference of 4.2 min. This gives some grounds for a positive assessment of

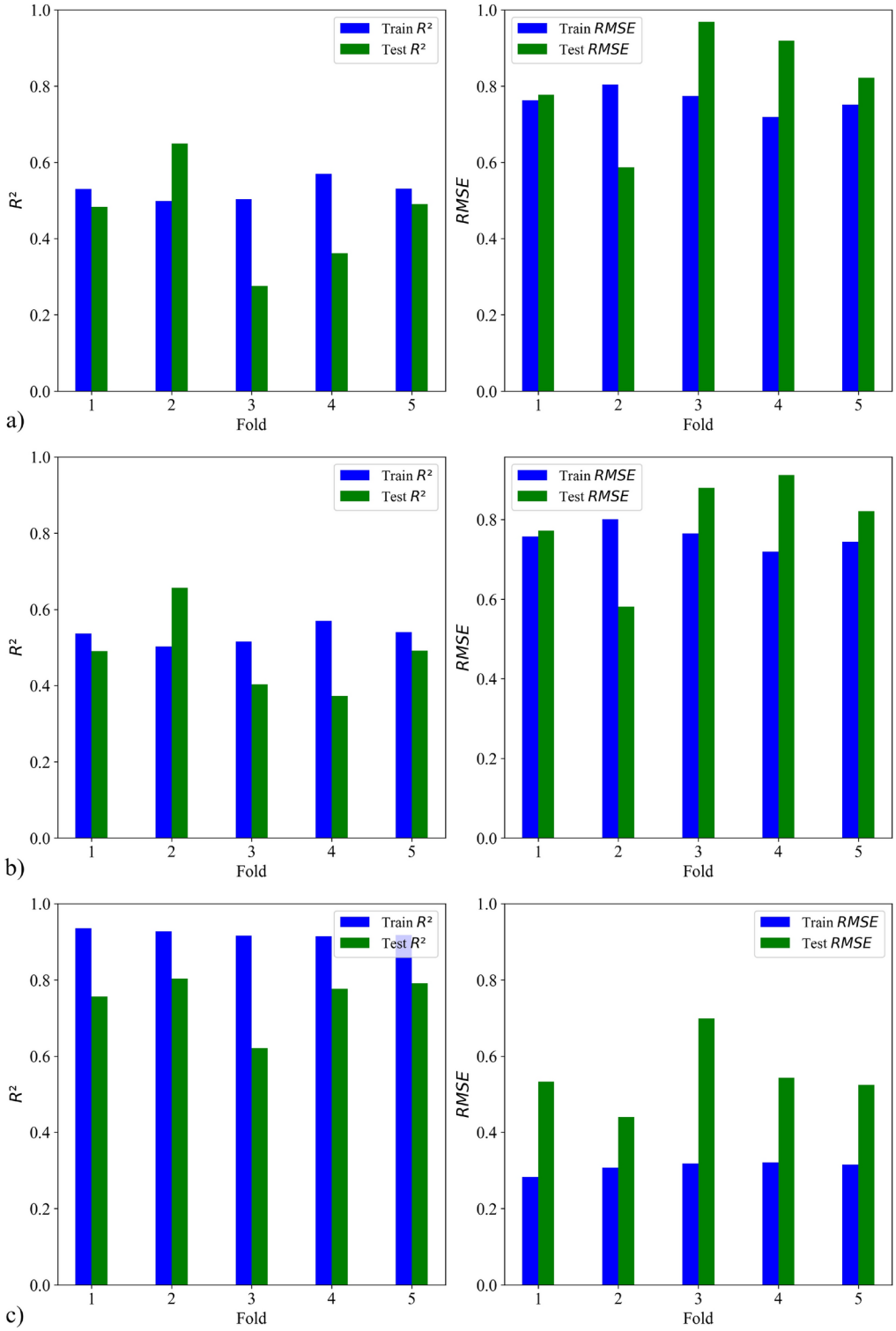

Figure 6. Performance metrics (R^2 and RMSE) comparison of six distinct ML: (**a**) Lasso regression, (**b**) ridge regression, (**c**) GPR, (**d**) SVR, (**e**) DT, and (**f**) RF algorithms utilizing 5-fold cross-validation.

the proposed creep life prediction method. Nevertheless, in the authors' opinion, the proposed algorithm still requires more training data, especially for long-term trials.

Conclusions

In summary, this research establishes a machine learning-based framework to accurately estimate the creep failure life of adhesive-bonded single-lap joints. The study primarily focuses on the role of mechanical properties

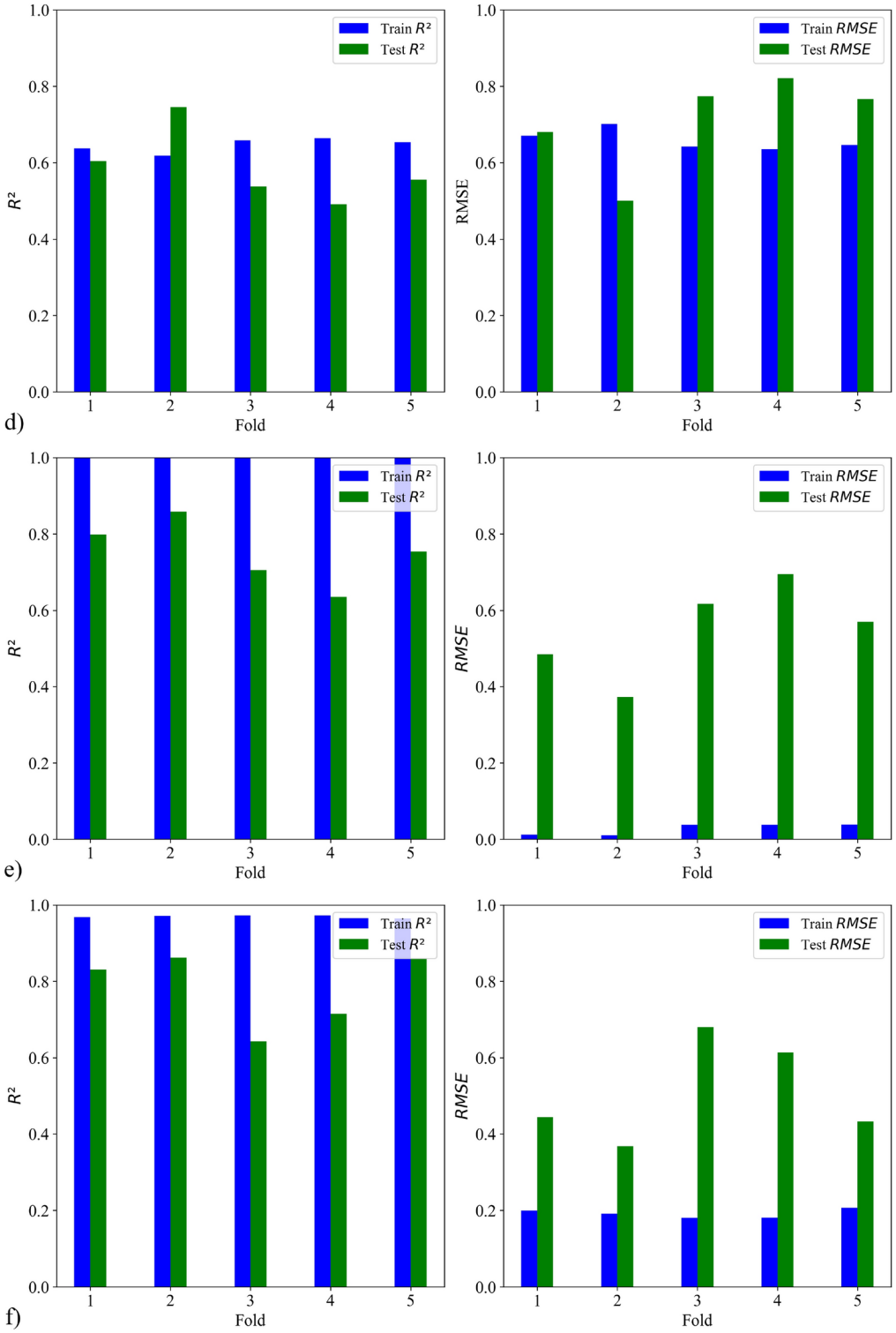

Figure 6. (continued)

in predicting the creep life of such joints. The developed feature screening method effectively identifies important attributes and reduces model complexity. This approach facilitates the identification of multiple significant factors that influence creep properties without extensive laboratory analysis. Incorporating additional features that affect creep life behavior into the dataset could further enhance the predictive performance of the creep failure life of adhesive-bonded SLJs. The primary conclusions can be formulate as follows:

- The data, gathered from multiple research papers, exhibited a very high standard deviation and a highly skewed distribution, attributed to the diversity of materials and test conditions used in compiling these val-

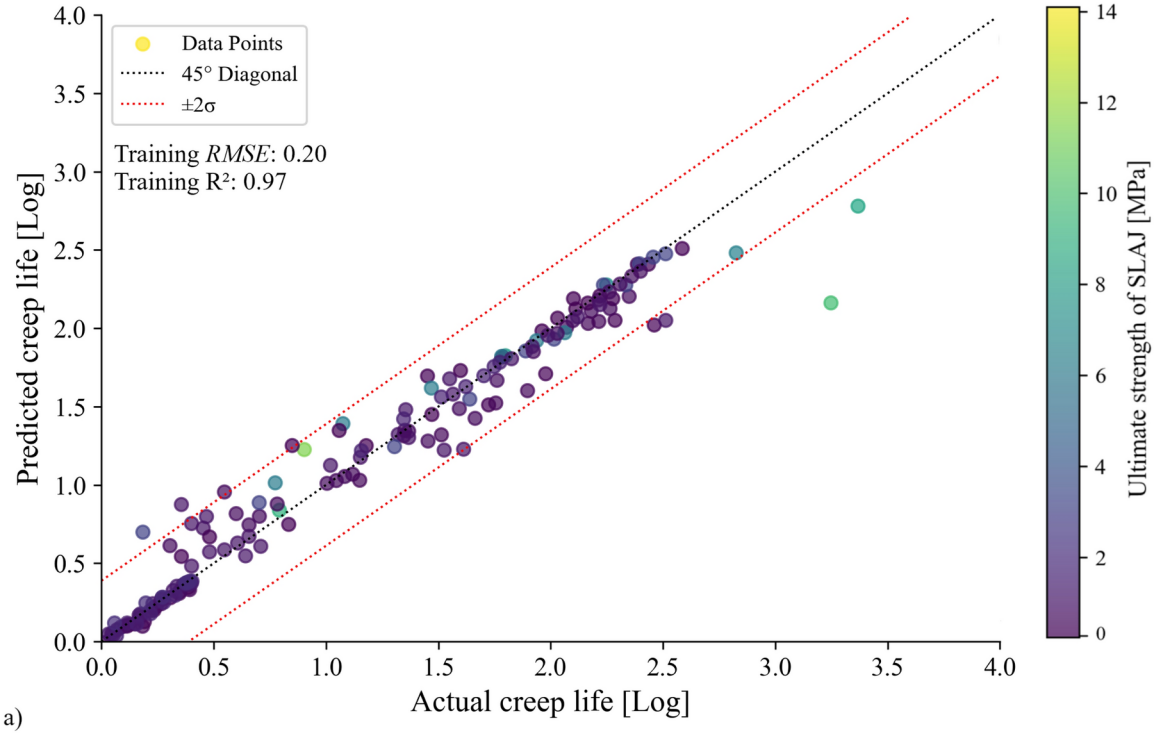

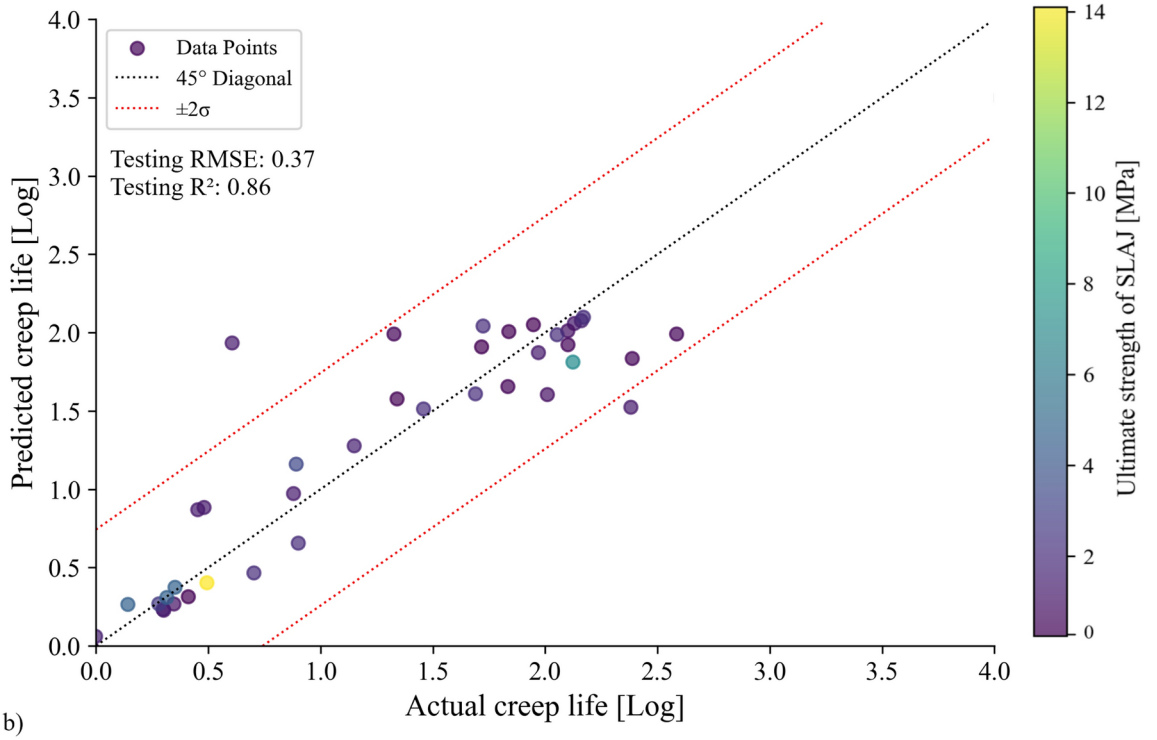

Figure 7. RF predictions for (**a**) training and (**b**) testing creep failure life on a logarithmic scale [Log].

ues. While this variability enables the representation of a broad spectrum of adhesive behaviors, it also poses challenges in developing highly accurate predictive models. Using unprocessed data directly in model construction could compromise prediction accuracy. To address this issue, a data normalization process was implemented to enhance modeling accuracy and facilitate data distribution analysis. Specifically, normalization was applied, transforming each variable into a range between 0 and 1 to ensure that no single variable dominated the model learning process. This approach also reduced the risk of algorithms converging on local minima. Comparative analyses of raw and normalized data demonstrated a significant improvement in model

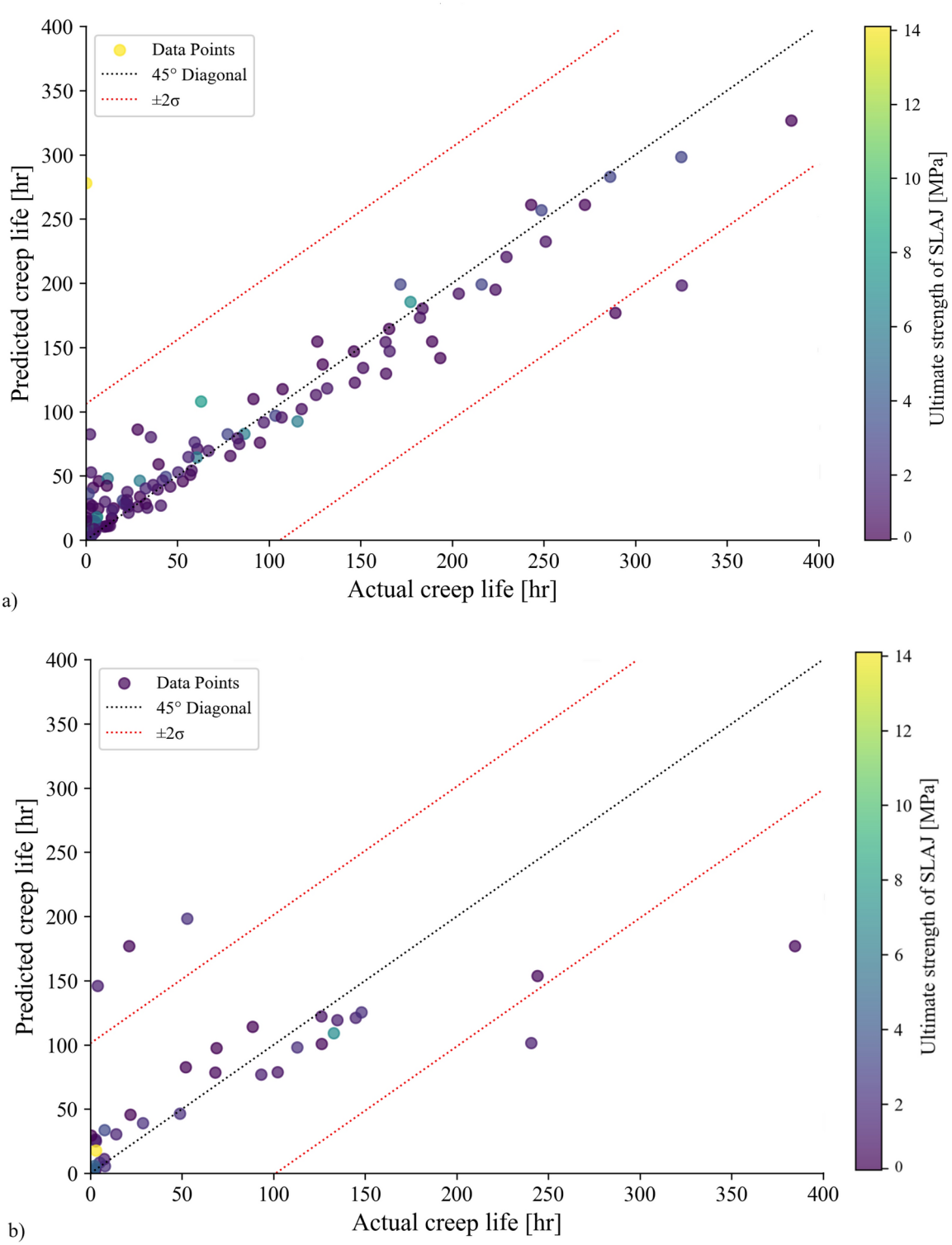

Figure 8. RF predictions for (**a**) training and (**b**) testing creep failure life on an actual scale [hr].

accuracy for the normalized dataset, underscoring the importance of data preprocessing in achieving more reliable predictions. Nevertheless, the authors acknowledge that the normalization process may have introduced certain limitations, such as potential distortions in the relationships between variables, which could affect the interpretability of the results. Additionally, it should be noted that the dataset does not represent the full population of available structural adhesives due to constraints in the availability of literature data and discrepancies in testing standards, which hinder complete homogenization of the results. The lack of a uniform measurement methodology in the literature may also have contributed to minor inaccuracies in the

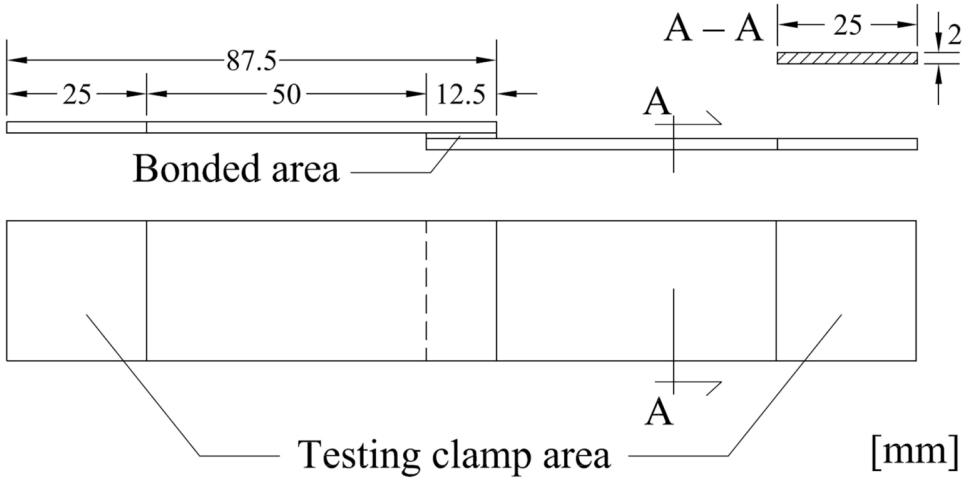

Figure 9. Shape and dimensions of the single-lap joints.

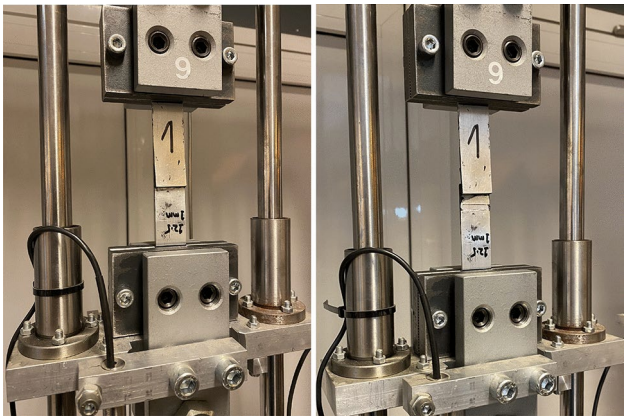

Figure 10. Creep test stand - the sample is subjected to a load of 3.0 kN (80% of failure load).

Abbreviation	Description	Min.	Max.	Mean	SD
USS [MPa]	Ultimate shear strength of SLAJ	11.40	11.85	11.65	0.230
UTS [MPa]	Ultimate tensile strength of adhesive	32.02	32.12	32.06	0.056
E [MPa]	Young's modulus of adhesive	1700	1743	1715	19.910
G [MPa]	Shear modulus of adhesive	625	622.5	621.4	9.850
ν [-]	Poisson's ratio of adhesive	0.36	0.40	0.38	0.010
Creep strain [-]	Creep strain of SLAJ	0.00018	0.002	0.0011	0.0006
Creep stress [MPa]	Creep stress of SLAJ	10.09	11.45	10.53	0.044
Temperature [°C]	Testing temperature	22	24	23	0.830
RH [%]	Relative humidity	45	60	55	5.250
t [mm]	Thickness of adhesive	1.19	1.23	1.21	0.020
A [mm^2]	Area of adhesive	264.50	300.00	288.45	10.55
Actual creep failure life [hr]	Time from creep to failure	0.04	15.69	**2.17**	5.47
Predict creep failure life [hr]	Time from creep to failure	0.72	7.40	**2.24**	2.89
Error	Relative error [%]			3.2	
	Absolute error [hr]			0.07	

Table 3. Experimental values of the selected features.

presented data. The authors are aware of these limitations and encourage cautious interpretation of the results, particularly when considering practical applications,

- Feature selection techniques and correlation analysis were employed to identify important features. Among eleven input features, five - including creep strain of SLAJ, creep stress of SLAJ, UTS of adhesive, Young modulus, and area of adhesive - were prioritized based on their importance for training the Random Forest model. The model trained with these five features achieved accuracy comparable to that of the model trained with all eleven input variables, underscoring the value of correlation analysis. The results from the correlation coefficient analysis revealed significant correlations between all features,
- Furthermore, it was found that the accuracy of the predictions made in this study is not significantly affected by characteristics linked to durability effects, such as test temperature and relative humidity. This is because the study primarily focuses on how mechanical parameters influence the prediction of creep failure life, independent of durability factors that might also be relevant. This demonstrates the effectiveness of the feature preprocessing used in this investigation,
- Among all the models trained using various machine learning techniques - including lasso, ridge regression, SVR, GPR, DT, and RF - the RF model, which utilized five essential features, made the most accurate predictions. The prediction accuracy of the RF model, which targets creep failure life, was assessed using 5 k-fold cross-validation, a critical method in machine learning. For the six models that exhibited excellent predictive ability, the mean R^2 value was calculated. Consequently, the RF model was found to have the most effective impact on predicting creep failure life among all the regression models. Furthermore, the model trained with creep failure life as the target feature demonstrated the best stability and accuracy.In conclusion, the current study successfully demonstrated the high efficiency and viability of integrating ML with knowledge of creep to predict the creep failure life of adhesive-bonded single-lap joints. It should be noted that proposed ML program code could be served as a useful tool for predicting creep failure life based on the mechanical characteristics of adhesive-bonded single-lap joints, but it has not yet fully elucidated the complex creep mechanisms of these joints under severe conditions that affect their longevity. Consequently, there is still considerable research to be done on the creep properties of adhesive-bonded single-lap joints under severe conditions. In future studies, one could explore the potential of combining clustering methods and correlation analysis in local modeling to predict properties alongside additional target features influenced by durability effects. Undoubtedly, further research is needed to investigate the effects of additional parameters, including extreme environmental factors over an extended period, on the creep behavior of bonded joints. Ultimately, addressing these challenges will not only refine predictive models but also enhance our understanding of the intricate behavior of adhesive-bonded joints, paving the way for more durable and reliable structural applications.

Data Availability

Additional data on which this paper has been developed can be found in the supplementary information files at: https://cloud.wilis.pg.edu.pl/index.php/s/8bMNdnMWkodtwjp. This data can be shared as a part of the pub lication of our paper.

Received: 8 October 2024; Accepted: 24 February 2025
Published online: 26 February 2025

References

1. Ramalho, L. D., Campilho, R. D., Belinha, J. & da Silva, L. F. Static strength prediction of adhesive joints: A review. *Int. J. Adhes. Adhes.* **96**, 102451 (2020).
2. Ciardiello, R., Greco, L., Miranda, M., Di Sciullo, F. & Goglio, L. Experimental investigation on adhesively bonded U-shaped metallic joints using the Arcan test. *J. Adv. Join. Process.* **1**, 100010 (2020).
3. Papanicolaou, G. C. & Zaoutsos, S. P. Viscoelastic constitutive modeling of creep and stress relaxation in polymers and polymer matrix composites. In *Creep and Fatigue in Polymer Matrix Composites*, Woodhead Publishing Series in Composites Science and Engineering, 3–59 (Elsevier, 2019).
4. Chen, Y. & Smith, L. V. A nonlinear viscoelastic-viscoplastic constitutive model for adhesives under creep. *Mech. Time-Depend. Mater.* **26**, 663–681 (2022).
5. Carneiro Neto, R. M., Akhavan-Safar, A., Sampaio, E. M., Assis, J. T. & da Silva, L. F. Effect of creep on the mode II residual fracture energy of adhesives. *J. Appl. Polym. Sci.* **138**, 51387 (2021).
6. da Silva, L. F., Öchsner, A. & Adams, R. D. (eds.) *Handbook of Adhesion Technology* (Springer, 2011).
7. Dillard, D. A. (ed.) *Advances in Structural Adhesive Bonding*. Woodhead Publishing in Materials (Woodhead Publishing, 2010).
8. Majda, P. & Skrodzewicz, J. A modified creep model of epoxy adhesive at ambient temperature. *Int. J. Adhes. Adhes.* **29**, 396–404 (2009).
9. Berrekheroukh, N., Sereir, Z., Vivet, A., Adda Bedia, E. A. & Fekrar, A. Experimental and numerical models to study the creep behavior of the unidirectional Alfa fiber composite strength by the photoelasticity method. *Mech. Time-Depend. Mater.* **26**, 547–564 (2022).
10. Ferry, J. D. *Viscoelastic Properties of Polymers* (Wiley, 1980).
11. Marques, E. A. S. et al. Use of master curves based on time-temperature superposition to predict creep failure of aluminium-glass adhesive joints. *Int. J. Adhes. Adhes.* **74**, 144–154 (2017).
12. Nkiwane, L. & Mukhopadhyay, S. K. Mathematical representation of creep for high-temperature performance of nylon6.6 tire materials. *J. Appl. Polym. Sci.* **72**, 1505–1511 (1999).
13. Mizah, B. R., Sekiguchi, Y. & Sato, C. Novel method to measure the creep strength of adhesively bonded butt joints subjected to constant loading using a hydro-pneumatic testing machine. *J. Adhes.* **92**, 65–79 (2016).
14. Marques, E. A. S., da Silva, L. F. M., Banea, M. D. & Carbas, R. J. C. Adhesive joints for low- and high-temperature use: An overview. *J. Adhes.* **91**, 556–585 (2015).
15. Feng, C.-W., Keong, C.-W., Hsueh, Y.-P., Wang, Y.-Y. & Sue, H.-J. Modeling of long-term creep behavior of structural epoxy adhesives. *Int. J. Adhesion Adhesive* **25**, 427–436 (2005).
16. Leaderman, H. *Elastic and Creep Properties of Filamentous Materials and Other High Polymers* (The Textile Foundation, Washington, 1943).

17. Shi, B., Yang, H., Liu, J., Crocetti, R. & Liu, W. Short- and long-term performance of bonding steel-plate joints for timber structures. *Constr. Build. Mater.* **240**, 117945 (2020).
18. Wang, J., Fa, Y., Tian, Y. & Yu, X. A machine-learning approach to predict creep properties of Cr-Mo steel with time-temperature parameters. *J. Market. Res.* **13**, 635–650 (2021).
19. Chai, M. et al. Machine learning-based framework for predicting creep rupture life of modified 9Cr-1Mo steel. *Appl. Sci.* **13**, 4972 (2023).
20. Burzyński, D. Useful energy prediction model of a Lithium-ion cell operating on various duty cycles. *Eksploatacja i Niezawodność - Maintenance and Reliability* **24**, 317–329 (2022).
21. Wang, C., Wei, X., Ren, D., Wang, X. & Xu, W. High-throughput map design of creep life in low-alloy steels by integrating machine learning with a genetic algorithm. *Mater. Des.* **213**, 110326 (2022).
22. Verma, A. K. et al. Mapping multivariate influence of alloying elements on creep behavior for design of new martensitic steels. *Metall. Mater. Trans. A.* **50**, 3106–3120 (2019).
23. Lin, L. et al. A machine learning method for soil conditioning automated decision-making of EPBM: Hybrid GBDT and Random Forest Algorithm. *Eksploatacja i Niezawodność - Maintenance Reliab.* **24**, 237–247 (2022).
24. Zhang, X.-C., Gong, J.-G. & Xuan, F.-Z. A deep learning based life prediction method for components under creep, fatigue and creep-fatigue conditions. *Int. J. Fatigue* **148**, 106236 (2021).
25. Mamun, O., Wenzlick, M., Sathanur, A., Hawk, J. & Devanathan, R. Machine learning augmented predictive and generative model for rupture life in ferritic and austenitic steels. *Mater. Degradat.* **5**, 20 (2021).
26. Liu, Y. et al. Predicting creep rupture life of Ni-based single crystal superalloys using divide-and-conquer approach based machine learning. *Acta Mater.* **195**, 454–467 (2020).
27. Han, H., Li, W., Antonov, S. & Li, L. Mapping the creep life of nickel-based SX superalloys in a large compositional space by a two-model linkage machine learning method. *Comput. Mater. Sci.* **205**, 111229 (2022).
28. Tan, Y. et al. Creep lifetime prediction of 9% Cr martensitic heat-resistant steel based on ensemble learning method. *J. Market. Res.* **21**, 4745–4760 (2022).
29. Shin, D., Yamamoto, Y., Brady, M. P., Lee, S. & Haynes, J. A. Modern data analytics approach to predict creep of high-temperature alloys. *Acta Mater.* **168**, 321–330 (2019).
30. Peng, J., Yamamoto, Y., Hawk, J. A., Lara-Curzio, E. & Shin, D. Coupling physics in machine learning to predict properties of high-temperatures alloys. *Comput. Mater.* **6**, 141 (2020).
31. Agrawal, A. et al. Exploration of data science techniques to predict fatigue strength of steel from composition and processing parameters. *Integr. Mater. Manuf. Innov.* **3**, 90–108 (2014).
32. Yan, F., Song, K., Liu, Y., Chen, S. & Chen, J. Predictions and mechanism analyses of the fatigue strength of steel based on machine learning. *J. Mater. Sci.* **55**, 15334–15349 (2020).
33. Hautier, G., Fischer, C. C., Jain, A., Mueller, T. & Ceder, G. Finding nature's missing ternary oxide compounds using machine learning and density functional theory. *Chem. Mater.* **22**, 3762–3767 (2010).
34. Gaultois, M. W. et al. Web-based machine learning models for real-time screening of thermoelectric materials properties. *APL Mater.* **4**, 053213 (2016).
35. Liu, R. et al. A predictive machine learning approach for microstructure optimization and materials design. *Sci. Rep.* **5**, 11551 (2015).
36. Yang, Z. et al. Deep learning approaches for mining structure-property linkages in high contrast composites from simulation datasets. *Comput. Mater. Sci.* **151**, 278–287 (2018).
37. Kumar, U., Nayak, S., Chakrabarty, S., Bhattacharjee, S. & Lee, S.-C. Gallium–Boron–Phosphide ($GaBP_2$): a new III-V semiconductor for photovoltaics. *J. Mater. Sci.* **55**, 9448–9460 (2020).
38. Li, J. et al. Accelerated discovery of high-strength aluminum alloys by machine learning. *Commun. Mater.* **1**, 73 (2020).
39. Queiroz, R. A., Sampaio, E. M., Cortines, V. J. & Rohem, N. R. F. Study on the creep behavior of bonded metallic joints. *Appl. Adhes. Sci.* **2**, 8 (2014).
40. Tan, W., Zhou, Z., Na, J. & Mu, W. Influence of temperature, humidity and load coupling on mechanical properties of adhesive joints and establishment of creep model. *Polymers* **15**, 339 (2023).
41. de Zeeuw, C. et al. Creep behaviour of steel bonded joints under hygrothermal conditions. *Int. J. Adhes. Adhes.* **91**, 54–63 (2019).
42. Duncan, B. C. & Ogilvie-Robb, K. Creep of flexible adhesive joints. Tech. Rep., NPL Report No.: CMMT(A)225 (1999).
43. Hiemer, S., Moretti, P., Zapperi, S. & Zaiser, M. Predicting creep failure by machine learning - which features matter?. *Forces Mech.* **9**, 100141 (2022).
44. Donate, J. P., Cortez, P., Sánchez, G. G. & de Miguel, A. S. Time series forecasting using a weighted cross-validation evolutionary artificial neural network ensemble. *Neurocomputing* **109**, 27–32 (2013).
45. Radhakrishnan, V. M. The relationship between minimum creep rate and rupture time in Cr-Mo steels. *J. Mater. Eng. Perform.* **1**, 123–128 (1992).
46. Browne, M. W. Cross-validation methods. *J. Math. Psychol.* **44**, 108–132 (2000).
47. Li, Z. et al. Machine learning in concrete science: applications, challenges, and best practices. *Comput. Mater.* **8**, 127 (2022).
48. Mahmood, A. & Wang, J.-L. Machine learning for high performance organic solar cells: current scenario and future prospects. *Energy Environ. Sci.* **14**, 90–105 (2021).
49. Lundberg, S. M. & Lee, S.-I. A unified approach to interpreting model predictions. In *NIPS'17: Proceedings of the 31st International Conference on Neural Information Processing Systems*, 4768–4777 (2017).

Acknowledgements

The paper is developed based on the statutory activity of the Poznan University of Technology (Grant of the Ministry of Science and Higher Education in Poland no 0612/SBAD/3628)

Author contributions

F.J. created the numerical code, M.K. and F.J. conceived the numerical and laboratory experiment(s), M.K., P.P. and F.J. conducted the laboratory experiment(s), M.K., P.P., F.J. and V.A.E. analysed the results. All authors reviewed the manuscript.

Declarations

Competing interests

The authors declare no competing interests.

Additional information

Supplementary Information The online version contains supplementary material available at https://doi.org/1

0.1038/s41598-025-91832-0.

Correspondence and requests for materials should be addressed to M.K.